SARS-CoV-2–Induced Vasculitic Skin Lesions Are Associated with Massive Spike Protein Depositions in Autophagosomes

JID Open

Andrea Gawaz[1], Michael Schindler[2], Elena Hagelauer[2], Gabriela Blanchard[3], Simon Riel[1], Anneli Vollert[1], Michel Gilliet[3], Luisa Unterluggauer[4], Georg Stary[4], Isabella Pospischil[5], Wolfram Hoetzenecker[5], Birgit Fehrenbacher[1], Martin Schaller[1], Emmanuella Guenova[3,6,7] and Stephan Forchhammer[1,7]

In patients infected with severe acute respiratory syndrome coronavirus 2, vasculopathic changes of the skin are associated with a severe prognosis. However, the pathogenesis of this vasculopathy is not conclusively clarified. In this study, 25 prospectively collected skin samples from patients with COVID-19–related skin lesions were examined for vasculopathic changes and, in case of vasculitis, were further analyzed with electron microscopy and immunohistochemistry. Vasculopathy was observed in 76% of all COVID-19–related inflammatory skin lesions. Visual endothelial changes without manifest leukocytoclastic vasculitis were found in 60% of the COVID-19–related skin lesions, whereas leukocytoclastic vasculitis was diagnosed in 16%. In the cases of vasculitis, there were extensive spike protein depositions in microvascular endothelial cells that colocalized with the autophagosome proteins LC3B and LC3C. The autophagy protein complex LC3–associated endocytosis in microvascular endothelial cells might be a contributing pathogenic factor for severe acute respiratory syndrome coronavirus 2–related vasculitis in the skin. On ultrastructural morphology, the vasculitic process was dominated by intracellular vesicle formation and endothelial cell disruption. Direct presence of severe acute respiratory syndrome coronavirus 2 particles in the skin was not observed. Therefore, our results suggest that instead of direct viral infection, dermal vasculitic lesions in COVID-19 might be related to severe acute respiratory syndrome coronavirus 2 spike protein deposition followed by endothelial damage with activation of autophagy.

Journal of Investigative Dermatology (2024) **144,** 369–377; doi:10.1016/j.jid.2023.07.018

INTRODUCTION

In the past 3 years, since its appearance in China, the novel coronavirus severe acute respiratory syndrome coronavirus 2 (SARS-CoV-2) has been studied intensely. COVID-19 was initially considered a disease of the respiratory tract. However, many studies have since shown the involvement of other organs, including the skin (Dou et al., 2020; Ertuğlu et al., 2020; Garrido Ruiz et al., 2021; Hernández-Fernández et al., 2020; Nuno-Gonzalez et al., 2021). In contrast to diseased internal organs, the inflammatory changes in the skin can be directly observed and easily biopsied. Cutaneous lesions occur in up to 20% of all patients with COVID-19 (Daneshgaran et al., 2020; Garrido Ruiz et al., 2021; Unterluggauer et al., 2021). Besides viral exanthema, vesicular or urticarial eruptions, chilblain-like skin lesions, vasculitic as well as livedo-like and vasculopathic changes, and ischemia have been reported (Galván Casas et al., 2020; Lange et al., 2022; Marzano et al., 2020a, 2020b; Shams et al., 2021).

The underlying pathology of these skin alterations is not yet entirely understood (Gawaz and Guenova, 2021; Zhao et al., 2020).

Initially, it was discovered that similar to severe acute respiratory syndrome coronavirus, SARS-CoV-2 exploits the angiotensin-converting enzyme 2 receptor for cell entry but binds with 10–20 times higher affinity (Wrapp et al., 2020). Entering the host cell requires the presence of both angiotensin-converting enzyme 2 receptor and cellular TMPRSS2 in the same cell type, such as in type II pneumocytes. However, a direct viral infection of skin endothelial cells could not yet be shown convincingly (Domizio et al., 2022).

Vasculopathic changes are strikingly frequent in SARS-CoV-2 infection and are related to worse prognosis of the disease (Becker, 2020).

[1]*Department of Dermatology, University Hospital Tübingen, Tübingen, Germany;* [2]*Institute for Medical Virology and Epidemiology of Viral Diseases, University Hospital Tübingen, Tübingen, Germany;* [3]*Department of Dermatology, Lausanne University Hospital (CHUV), Faculty of Biology and Medicine, University of Lausanne, Lausanne, Switzerland;* [4]*Department of Dermatology, Medical University of Vienna, Vienna, Austria;* [5]*Department of Dermatology, Kepler University Hospital, Johannes Kepler University, Linz, Austria; and* [6]*Department of Dermatology, Hospital 12 de Octubre, Medical school, University Complutense, Madrid, Spain*

[7]*These authors contributed equally to this work.*

Correspondence: Emmanuella Guenova, Department of Dermatology, Lausanne University Hospital (CHUV), Faculty of Biology and Medicine, University of Lausanne, Avenue de Beaumont 29, Lausanne 1011, Switzerland. E-mail: emmanuella.guenova@unil.ch

Abbreviation: SARS-CoV-2, severe acute respiratory syndrome coronavirus 2

Received 19 May 2023; revised 21 July 2023; accepted 24 July 2023; accepted manuscript published online 12 August 2023; corrected proof published online 7 November 2023

It has been shown that SARS-CoV-2 viruses can affect both cell metabolism and autophagy pathways (Gassen et al., 2021). This leads to an accumulation of key metabolites, including the autophagy marker LC3B, in infected cells. Recently, LC3B was shown to function as an RNA-binding protein that triggers mRNA degradation during autophagy (Hwang et al., 2022). Therefore, a further aim of our study was to determine whether changes in LC3-associated autophagy can also be observed in cutaneous vasculitis in the setting of COVID-19 infection.

RESULTS

Frequency of endothelial injury in COVID-19–related inflammatory skin lesions

Twenty-five prospectively recruited patients with COVID-19–related maculopapular, vesiculopapular, and purpuric–necrotic skin lesions and three patients with leukocytoclastic vasculitis from four European centers—one in Germany, one in Switzerland, and two in Austria—were included in this study. COVID toes were not part of this analysis. Supplementary Table S1 summarizes the cohort's demographic characteristics, comorbidities, and course of disease. Age distribution in the study group ranged from 19 to 67 years, with a median age of 43 years. Fifteen of the patients with COVID-19 were male, and 10 were female. In total, vasculopathic changes and endothelial injury were very common in COVID-19–related inflammatory skin lesions and could be detected in 76% of all cases (n = 19 of 25). Histological diagnosis of leukocytoclastic vasculitis was made in 16% of all cases (n = 4 of 25), whereas visual endothelial changes without manifest leukocytoclastic vasculitis were found in 60% of the cases (n = 15 of 25). All vasculitic lesions were dissected ultrastructurally for microvascular and endothelial damage, mechanisms of vascular injury, and the presence of SARS-CoV-2 viral particles in the skin.

Clinical and histological characteristics of SARS-CoV-2–related vasculitic skin lesions

The four skin lesions with leukocytoclastic vasculitis concomitant to COVID-19 disease were biopsied in four different patients from our prospective cohort: two males and females, aged between 21 and 62 years (Figure 1a and b). All patients molecularly tested positive for SARS-CoV-2 and developed skin symptoms, concomitant to their COVID-19 infection. Three of them had a mild course of the disease. The fourth patient was a male individual aged 22 years, who was otherwise healthy. He experienced a severe COVID-19 disease course and developed myocarditis with subsequent heart failure that necessitated extracorporeal membrane oxygenation. In brightfield microscopy, the vascular endothelial damage and the concomitant inflammation pattern in all four SARS-CoV-2–related vasculitic skin lesions were similar and resembled closely the pathology of classical leukocytoclastic vasculitis. We observed vasocentric lymphohistiocytic and neutrophilic inflammatory infiltrates, neutrophilic nuclear dust, erythrocyte extravasation, and degeneration of capillary vessel walls with fibrin deposition (Figure 1c). Table 1 documents the semiquantitative evaluation of the histological changes.

Ultrastructural characteristics of the vascular injury in SARS-CoV-2–related vasculitic skin lesions

We next performed electron microscopy for ultrastructural characterization of the capillaries and the endothelial damage and to interrogate causality of direct viral presence in the skin. As in brightfield microscopy, the ultrastructural pattern of vascular damage in all four SARS-CoV-2–related vasculitic skin lesions remained similar. First and most important, no SARS-CoV-2 viral particles could be detected in any of the analyzed COVID-19–related skin samples. Molecular analysis (PCR) of the skin samples showed an absence of SARS-CoV-2 virus in the lesional skin. However, all vasculitic skin lesions from patients with COVID-19 were characterized by the presence of multiple severely damaged dermal capillaries with development of numerous intracytoplasmic vesicles and autophagosomes in injured endothelial cells (overview in Figure 2a and b). Furthermore, we detected partial cellular destruction of nonendothelial cells localized in the proximity of the vascular damage (vascular-associated cells) (Figure 2e). Interestingly, those vascular-associated cells

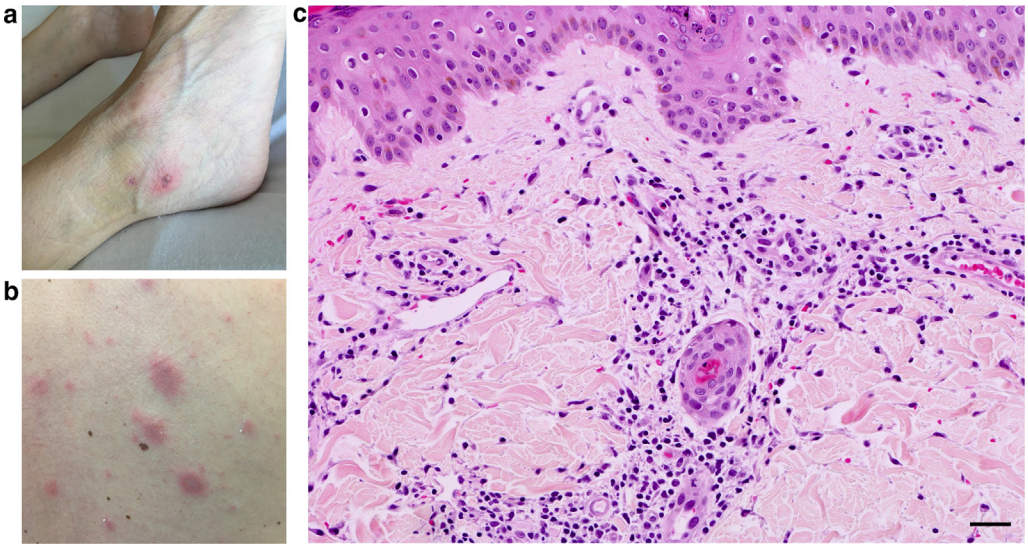

Figure 1. SARS-CoV-2–related vasculitic skin lesion. (**a, b**) Clinical images. (**c**) H&E-stained skin punch biopsy from patient's back. Bar = 50 μm. SARS-CoV-2, severe acute respiratory syndrome coronavirus 2.

Table 1. Histological Characteristics of Patients (1−4) and Controls (n = 3)

Characteristics	Patient 1	Patient 2	Patient 3	Patient 4	Vasculitis
Histology					
Epidermal necrosis	++	−	−	−	−
Vasocentric lymphohistiocytic infiltration	+	+	++	+	+
Vasocentric neutrophilic infiltration	+	++	+	+	+++
Neutrophilic nuclear dust	++	+	+	+	+++
Erythrocyte extravasation	++	+	++	+	++
Fibrin deposits in vessel walls	++	+	+	−	++
Papillary body vasculitis	+	++	+	+	+
Immunohistochemistry					
MPO neutrophils	+	+	+	+	+++
LL37 neutrophils	+	+	−	+	+++
LL37 vessel-associated cells	++	−	++	+	−
IgG connective tissue	+	+	++	+	−
IgG vessel-associated cells	+	+	+	+	−
IgG endothelial cell	+	+	+	+	++
VEGF nucleus	++	++	++	+	−
VEGF cytoplasm	+	+	+	+	+
LC3B	++	+	+	+	−
LC3C	++	+	++	+	−
Spike protein	+	+	++	+	−
CD163 (macrophages)	+	+	+	+	−
Electron microscopy					
Loss of nuclear structure	+	+	+	+	n/a
Autophagosomes	++	++	++	+	n/a
Virus particles	−	−	−	−	n/a
Endothelial cell damage	++	−	+	−	n/a
Vascular environment cell damage	−	++	−	+	n/a

Abbreviations: MPO, myeloperoxidase; n/a, not applicable.

developed a cytoplasmatic phenotype similar to that of endothelial cells (Figure 2f). Ultrastructural analysis of the cell nuclei of both injured endothelial and vascular-associated cells revealed loss of the typical normal heterochromatin and euchromatin structure (Figure 2c). Small thrombi, consisting of degranulated platelets and fibrin, could be detected inside the wall of many of the damaged vessels (Figure 2d).

Finally, for reference of SARS-CoV-2−induced type of cellular damage, we assessed the ultrastructural characteristics of SARS-CoV-2−infected Calu-3 lung adenocarcinoma cells (Figure 3a). To our expectations, in cells from the infected Calu-3 cell line, we observed a similar destructive pattern and a considerable amount of autophagosomes (Figure 3b).

However, in contrast to human COVID-19−related skin lesions, in SARS-CoV-2−infected Calu-3 lung adenocarcinoma cell line, SARS-CoV-2 viral particles (Figure 3c) and virus factories were easily detectable as signs of active viral replication (Figure 3d).

SARS-CoV-2 spike protein colocalizes with major autophagy proteins LC3B and LC3C in vasculitic COVID-19 skin disease

Multiple autophagosomes in both endothelial and vascular-associated cells were our major ultrastructural finding in vasculitic COVID-19 skin disease. To further elucidate the mechanism of vascular injury, we compared serial sections from clinical samples with cutaneous vasculitis from patients with or without SARS-CoV-2 infection (i.e., classical leukocytoclastic vasculitis lesions sampled before the outbreak of the COVID-19 pandemic). Healthy skin samples or SARS-CoV-2−infected Calu-3 lung adenocarcinoma cell lines served as positive and negative controls, respectively. Autophagy is a cellular process involved in the recycling and degradation of cellular components, and the LC3 family of proteins is commonly used as markers for autophagy (Khandia et al., 2019). LC3B is ubiquitously expressed in various tissues and cell types. LC3A is also widely expressed but less common in the skin. LC3C, expressed at lower levels, has been linked to viral-related autophagosome formation (Madjo et al., 2016; Maier et al., 2013). We focused our analysis on LC3B and LC3C proteins (Coelho et al., 2022). Both LC3B and LC3C were present in our samples with vasculitic COVID-19 skin disease. In particular, LC3B detection was more prominent in the areas of vascular-associated cells, whereas LC3C was more evident directly in the endothelial cells of the small cutaneous vessels (Supplementary Figure S1). In control samples from healthy skin, neither LC3B nor LC3C was detectable in any vascular or perivascular structures (Supplementary Figure S2). Of note, although SARS-CoV-2 viral particles were indetectable in human skin from patients with COVID-19, we observed abundant SARS-CoV-2 spike proteins located both in the cytoplasm and in/around the nucleus of endothelial cells of the dermal capillaries (Figure 4a and b). These depositions of the SARS-CoV-2 spike proteins colocalized to a great extent with the autophagy proteins LC3B and LC3C (Supplementary Figure S1). In addition, we detected IgG depositions throughout the vascular environment. VEGF was found intranuclear and intracytoplasmic as a further marker of endothelial cell damage (Figure 4c). The histological detection of polymorphonuclear neutrophilic granulocytes in brightfield microscopy (Figure 1c) correlated well and as expected with massive perivascular accumulation of the neutrophil-derived myeloperoxidase and LL37 proteins (Figure 4d).

Vasculitic COVID-19 skin disease differs from classical leukocytoclastic vasculitis in the skin

Analysis of vasculitic lesions unrelated to SARS-CoV-2 revealed that in clinical samples from classic leukocytoclastic vasculitic lesions (cutaneous vasculitis from patients without SARS-CoV-2 infection), neither SARS-CoV-2 spike proteins nor the autophagy proteins LC3B and LC3C were detected (Supplementary Figure S3a and b). Interestingly, on the level of immune depositions, vasculitic COVID-19 skin disease differed substantially from classical leukocytoclastic vasculitis in the skin. In contrast to the image observed in COVID-19 skin vasculitis, in leukocytoclastic skin vasculitis, we found IgG depositions exclusively inside the endothelial

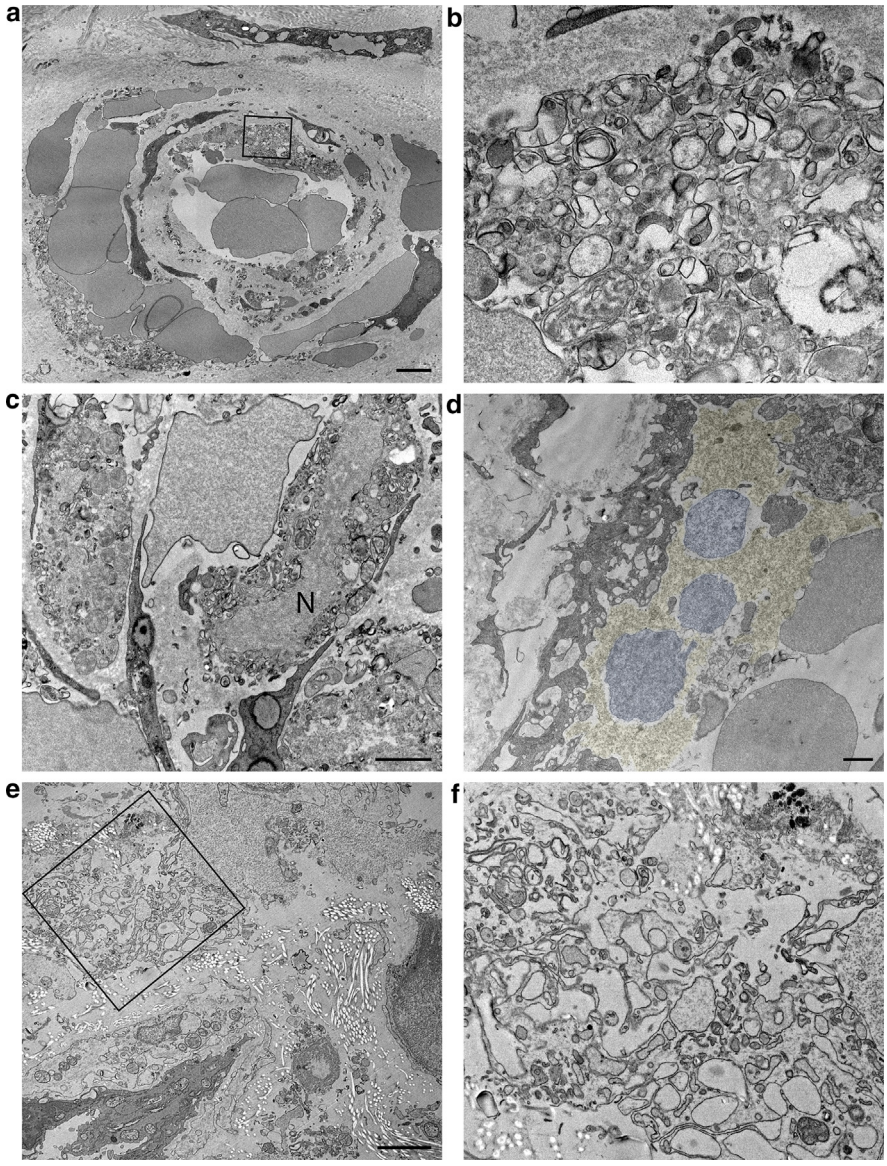

Figure 2. Transmission electron microscopy of dermal microvascular cells in skin biopsies from patients with COVID-19. (**a**) Overview of a damaged skin vessel. (**b**) Square in **a** shows cytoplasm at higher magnification. (**c**) Microenvironment of the same vessel in a serial section. (**d**) Thrombus in a vessel wall (platelets blue, fibrin yellow). (**e**) Intact endothelial cell and damaged microenvironment; (**f**) square in **e** shows cytoplasm at higher magnification. Bar in **a** and **e** = 2 μm and **c** and **d** = 1 μm.

cells, and VEGF detection was limited to the cytoplasm (Supplementary Figure S3c). Next, the inflammatory infiltrate of leukocytoclastic vasculitic skin lesions contained a much higher number of polymorphic neutrophilic granulocytes; furthermore, the neutrophilic-derived antimicrobial peptide LL37 was detected in the nucleus, unlike in COVID-19 vasculitis where it was found in the cytoplasm (Supplementary Figure S3d).

Calu-3 lung adenocarcinoma cells show the same response as in vasculitic COVID-19 disease

As a reference, Calu-3 lung adenocarcinoma cells were infected with SARS-CoV-2 (Deinhardt-Emmer et al., 2021) or treated with supernatant from SARS-CoV-2 spike protein–expressing cells and stained with antibodies against LC3B, LC3C, and SARS-CoV-2 spike proteins. As in our human samples, all virus-infected cells expressed the autophagy-related proteins LC3B and LC3C, with half of the cells also expressing SARS-CoV-2 spike protein. Different from virus-infected cells, Calu-3 cells exposed to the supernatant from SARS-CoV-2 spike protein–expressing cells were LC3B positive but remained LC3C negative. SARS-CoV-2 spike protein was present in most cells, also in the nucleus in some cases (Figure 5).

DISCUSSION

A variety of skin changes, including vasculopathy, have been reported in COVID-19–related disease. In this study, we dissect the morphological, immunohistochemical, and ultrastructural changes due to cutaneous vasculitis in the context of SARS-CoV-2 infection. In a cohort of 25 prospectively collected clinical samples from COVID-19–related inflammatory skin lesions, vasculopathy was common (76%), and vasculitis was present in 16% of all cases. Direct presence of SARS-CoV-2 virus particles in the skin was not observed. Instead, SARS-CoV-2 spike protein colocalizes with two major autophagy proteins LC3B and LC3C specifically in vasculitic COVID-19 skin disease but not in non–SARS-CoV-2–related leukocytoclastic vasculitis, indicating

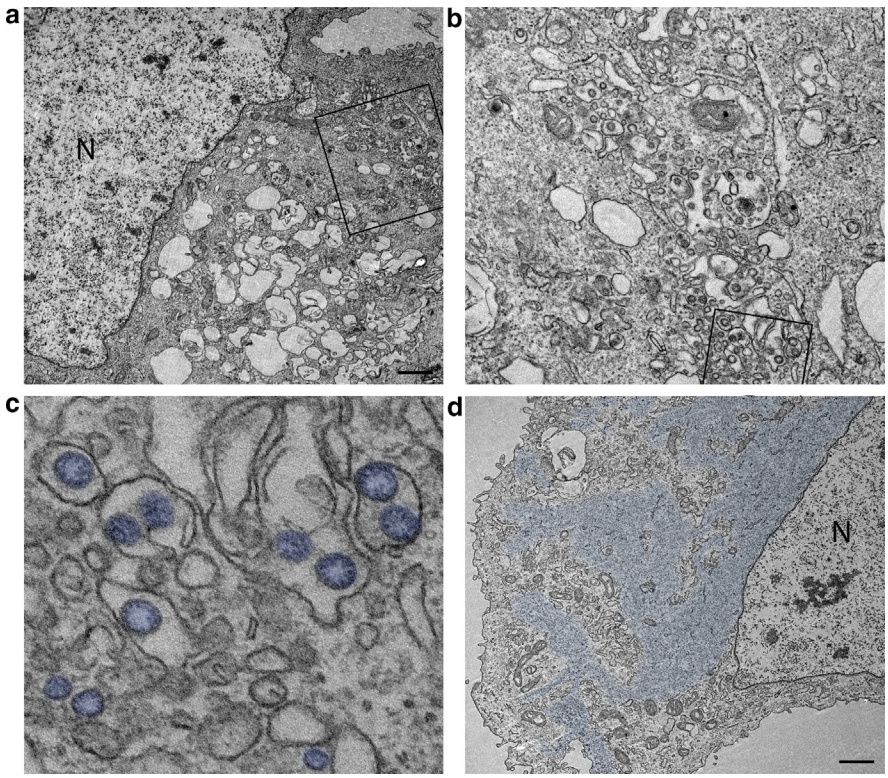

Figure 3. Transmission electron microscopy of Calu-3 cells infected with SARS-CoV-2. (**a**) Overview of an isolated Calu-3 cell; square in **a** shows higher magnification in **b**, and square in **b** shows higher magnification in **c** with SARS-CoV-2 virus particles (blue). (**d**) Virus factory (blue). Bar in **a** and **d** = 1 μm. SARS-CoV-2, severe acute respiratory syndrome coronavirus 2.

spike-induced autophagy as a relevant mechanism for COVID-19–related vasculitis. In addition, immune deposition profile of vasculitic COVID-19 skin disease was distinct and different from that of classical leukocytoclastic vasculitis in the skin. In particular, the SARS-CoV-2–related vasculitic pattern was identical in all skin lesions included in our analysis, independent of the differences in the clinical appearance of the skin lesions and the overall severity of the systemic disease. On classical histological level, the COVID-19–related vasculitic skin lesions in all our patients resembled leukocytoclastic vasculitis but had fewer neutrophil granulocytes and less nuclear dust in the inflammatory infiltrate. A specific noticeable feature was the accentuation of the inflammatory reaction in the papillary dermis, a finding that has been observed and reported by others as well (Caputo et al., 2021; García-Gil et al., 2020; Negrini et al., 2020).

In COVID-19 vasculitis, we detected extensive spike protein deposition in the capillary endothelia of the skin. It is an ongoing discussion whether these spike protein deposits are the result of direct infection with SARS-CoV-2 or the consequence of circulating spike protein from perished lung epithelial cells that were taken up into microvascular endothelial cells. Previous studies report evidence of direct viral infection of various tissues and organs (Bradley et al., 2020; Dolhnikoff et al., 2020; Facchetti et al., 2020; Farkash et al., 2020; Varga et al., 2020). In addition, two publications have described ultrastructural detection of putative SARS-CoV-2 viruses in endothelial cells of the skin (Colmenero et al., 2020; Garrido Ruiz et al., 2021). What renders the discussion and correct interpretation of the findings even more complicated is the fact that several different cell types could be infected with SARS-CoV-2 in vitro (Bartolomeo et al., 2022; Gassen et al., 2021). However, electron microscopic imaging of viruses is not without controversy, because viruses may be easily confused with other structures of the cell, such as coated vesicles or rough endoplasmic reticulum (Bradley et al., 2020; Hopfer et al., 2021). In the end, most of the alleged virus evidence does not stand up to scrutiny (Dittmayer et al., 2020; Dittmayer and Laue, 2022; Hopfer et al., 2021).

Despite intensive investigation, we could not detect SARS-CoV-2 virus particles in the skin by electron microscopy. It cannot be excluded with absolute certainty that the time of sample collection was too late. Dittmayer et al. (2020) demonstrated intact SARS-CoV-2 virus particles in the lung endothelial cells with a postmortem interval of 30 hours. In our study, biopsies were taken between 2 and 4 days after the appearance of the skin symptoms, so that transient virus presence may no longer be detected.

Although PCR testing for viral RNA has a high sensitivity and specificity in the detection of SARS-CoV-2 in tissue, this test was deliberately omitted. Because the crucial question of our work was the localization of the possible infection, especially the detection or absence of intact virus particles in endothelial cells, this could not be answered by PCR (Roden et al., 2021).

Endothelial dysfunction, the main pathology in COVID-19, is assumed to be multifactorial in origin, centered on innate immune mechanisms such as the activation of the complement system or the cGAS–STING pathway with pathological type I IFN response (Domizio et al., 2022). It has been shown that activation of the STING pathway also activates NF-κB and enhances the formation of LC3$^-$positive vesicles (Decout

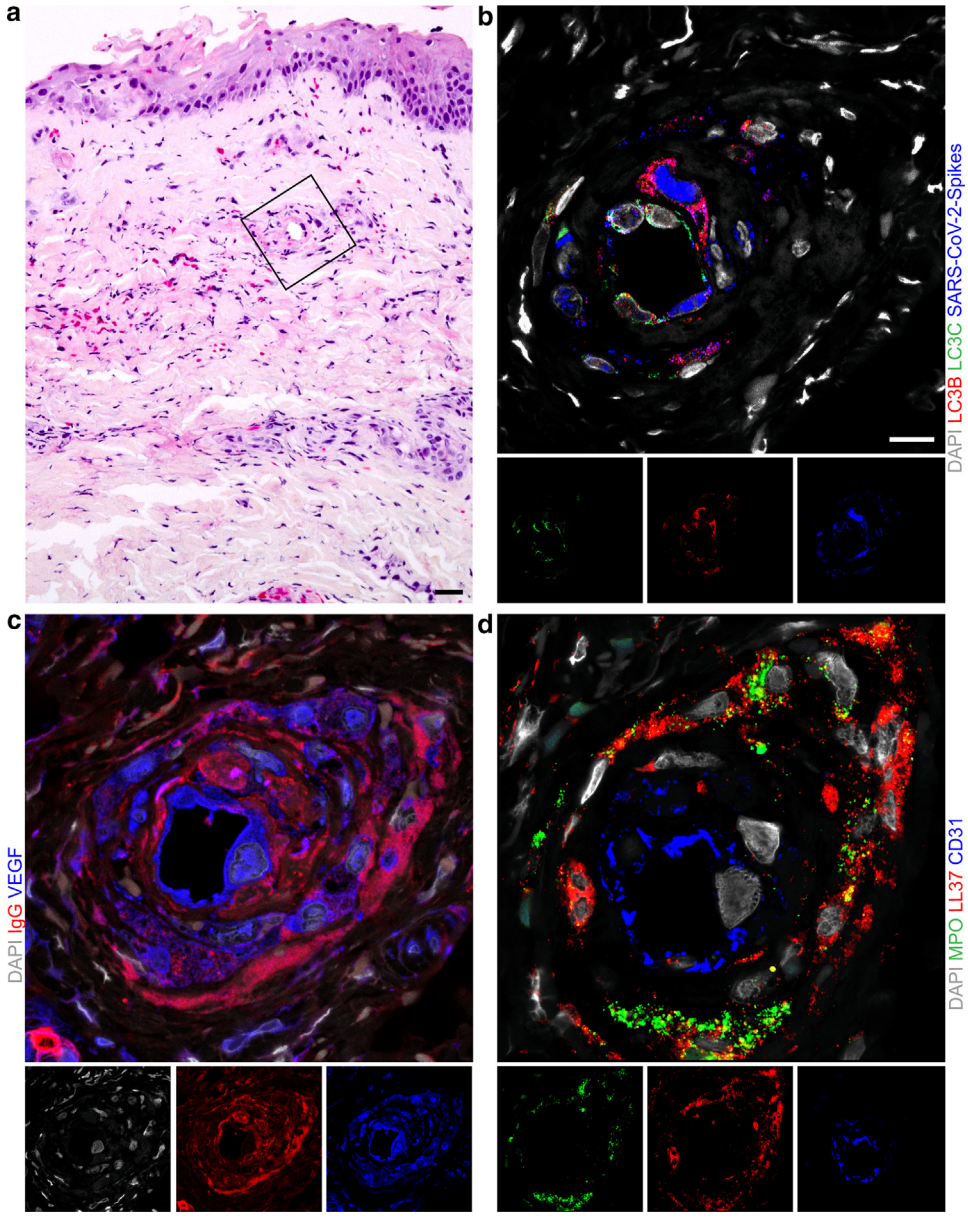

Figure 4. Dermal microvascular cells in COVID-19. Representative serial sections of one COVID-19 skin sample with diverse stainings. (**a**) H&E overview, square marking the same vessel seen in **b**, **c**, and **d**. (**b**) LC3B (red), LC3C (green), SARS-CoV-2 spikes (blue). (**c**) IgG (red) and VEGF (blue). (**d**) MPO (green), LL37 (red), and CD31 (blue). DAPI (gray) was used for nuclear staining (in **b**–**d**). Bar in **a** = 10 μm **b** = 50 μm. MPO, myeloperoxidase; SARS-CoV-2, severe acute respiratory syndrome coronavirus 2.

et al., 2021). In our study, we found evidence of endotheliitis with a strong inflammatory reaction in the upper dermis. Electron microscopy demonstrated endothelial cells with loss of cell structure that were filled with numerous vesicles. Moreover, there was extensive deposition of spike protein and LC3 in these cells, which may be an indicator of LC3-associated endocytosis (Bischoff et al., 2021). For SARS-CoV-2, Gassen et al. (2021) showed distinct inhibition of autophagy pathways with a reduction of several proteins that regulate autophagy in SARS-CoV-2–infected cells, which subsequently causes accumulation of LC3B in affected cells in vitro.

Immunohistochemical staining of LL37 shows a differential expression in COVID-19–associated vasculitis in contrast to classical leukocytoclastic vasculitis. Although cases of classical leukocytoclastic vasculitis showed expression in the nucleus, the protein was predominantly found in the cytoplasm in COVID-19–associated cases. Migration of LL37 into the nucleus was reported in overwhelming infections (Pinheiro da Silva et al., 2013). The fact that cytoplasmic and not nuclear detection was possible in our patients with COVID-19–associated vasculitis might indicate that there is no direct infection of the endothelia in SARS-CoV-2–related vasculitis.

The presence of SARS-CoV-2 spike protein in microvessels of different organs, including the skin, has been confirmed in numerous studies (Colmenero et al., 2020; Ko et al., 2021; Magro et al., 2020; Welsh et al., 2022). It has been hypothesized that the spike protein itself may lead to complement activation and subsequently to a prothrombotic state, which is typical for severe COVID-19 cases (Magro et al., 2021). Another explanation for the multiple vesicles found in endothelial cells would be that of immunological deception. The release of virosomes that act as decoys to block neutralizing antibodies has been described for Ebola and hepatitis B viruses (Hu and Liu, 2017; Nehls et al., 2019)

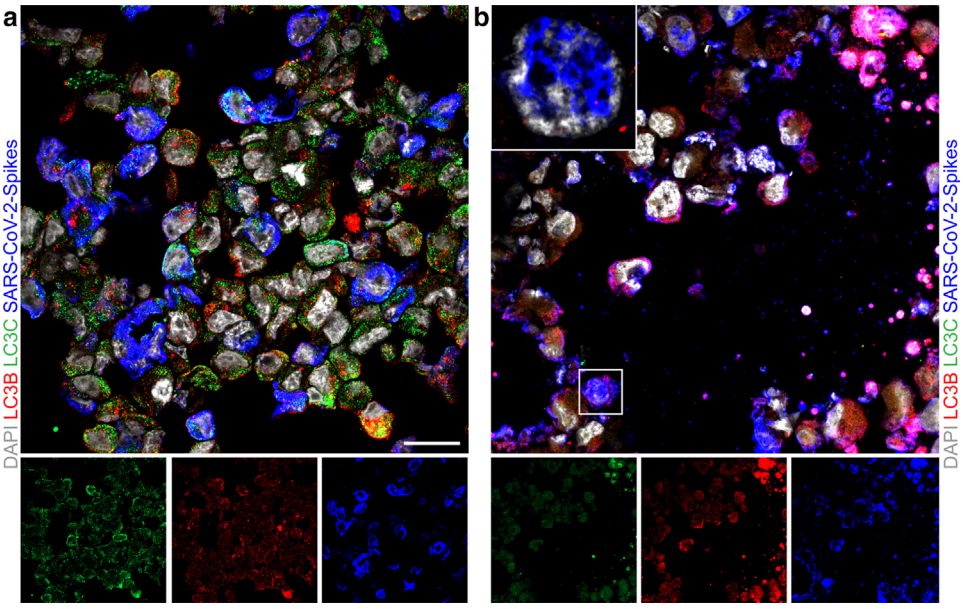

Figure 5. Confocal immunofluorescence—Calu-3 cells. (**a**) Representative sections of SARS-CoV-2 and (**b**) spike protein–containing supernatant–treated Calu-3 cells stained for LC3B (red), LC3C (green), and SARS-CoV-2 spikes (blue). Nuclei were stained with DAPI (gray). The insert in **b** shows a magnification of nuclear SARS-CoV-2 spikes. Bar in **a** = 20 μm. SARS-CoV-2, severe acute respiratory syndrome coronavirus 2.

Our study has some limitations. One major limitation is the small sample size. Possibly, in a larger cohort, more aspects of vasculitic injury could be represented, which may not be captured in this study. Another limitation is the timing of sample collection. We only had samples from one time point for each patient. It is possible that changes, which are only transient, were not recorded. Even a direct viral infection, which can possibly only be detected in a narrow time frame, cannot be ruled out with absolute certainty. Another limitation is that we did not have a serum sample from the patients at the time of the disease. Possible detection of spike protein in serum could therefore not be performed.

In summary, our study demonstrates a possible explanation of vascular cell damage in the skin in COVID-19–related vasculitis. Our data support the hypothesis that this is not a consequence of direct viral infection but a SARS-CoV-2 spike protein–associated inflammatory process.

PATIENTS AND METHODS

Clinical samples

Clinical samples, images, and related metadata were retrieved from prospectively collected and biobanked residual material from patients with COVID-19–related skin disease or leukocytoclastic vasculitis treated at the Lausanne University Hospital (Lausanne, Switzerland), the Kepler University Hospital (Linz, Austria), the Vienna University Hospital (Vienna, Austria), and the University Hospital Tuebingen (Tuebingen, Germany). Patients provided written informed consent. The sample acquisition was approved by the local ethics authorities (CER-VD2021-00878, CER-VD2020-02204, #1392/2020-Linz, 089/2023BO2). The diagnosis of COVID-19 was based on a positive nasal swab for SARS-CoV-2 and matching clinical symptoms. Formalin-fixed samples were available from all patients. Glutaraldehyde-fixed samples for further electron microscopic processing were available from 9 of the 25 patients. Only the samples that showed vasculitic changes in histology were further processed by electron microscopy and immunohistochemistry. For non–COVID-19–related leukocytoclastic vasculitis and for normal skin as a negative control, only patient samples acquired before the beginning of the COVID-19 pandemic in 2020 were used.

Histology

Formalin-fixed and paraffin-embedded tissue was cut into 3-μm thick sections, deparaffinized, and stained with H&E following standard procedures. The sections were examined for vasculopathy and vasculitic changes by board-certified dermatopathologists. The presence of vasculitis was defined by the presence of angiocentric or angioinvasive inflammatory infiltrates, destruction of the vessel wall, and intramural or intraluminal fibrin deposition (Carlson, 2010). The histological sections of the patients were evaluated semi-quantitatively by a dermatopathologist for the presence of an epidermal necrosis zone, vasocentric infiltrates, neutrophil nuclear dust, erythrocyte extravasations, fibrin deposit, and vasculitis in the area of the papillary bodies. In this study, a classification was made in four gradations (−, +, ++, and +++).

Transmission electron microscopy

For electron microscopic analyses, SARS-CoV-2–infected Calu-3 cells (Tü1, described in the study by Ruetalo et al. (2021); multiplicity of infection of 0.06; 36-hour infection) were fixed in Karnovsky's solution. After centrifugation, the sediment was embedded in 4% agarose (Sigma-Aldrich, St. Louis, MO) at 37 °C, cooled on ice, and stored in Karnovsky's solution. Skin biopsies were fixed in Karnovsky's solution, and subsequently, both Calu-3 cells and biopsies were post-fixed with 1.0% osmium tetroxide containing 1.5% K-ferrocyanide in 0.1 M cacodylate buffer for 2 hours. Samples were rinsed with distilled water, block stained with uranyl acetate (2% in distilled water), dehydrated in alcohol (stepwise 30–96%), immersed in propylene oxide, embedded in glycidyl ether (polymerized for 48 hours at 60 °C; Serva Serva Electrophoresis, Heidelberg, Germany), and cut using an ultramicrotome (Ultracut). Semithin sections were stained with toluidine blue (1% Morphisto) and examined for initial orientation under a Nikon eclipse 80i microscope (Nikon Europe BV, Amstelveen, The Netherlands).

Subsequently, pathologically altered or interesting regions with a focus on vessels were selected and retrimmed for ultrathin

sectioning. Ultrathin sections (30 nm) were mounted on copper grids, and the areas in and around each vessel were inspected for SARS-CoV-2, along with the eccrine glands of one patient. A Zeiss LIBRA 120 transmission electron microscope (Carl Zeiss, Oberkochen, Germany) was used for the analysis, operating at 120 kV.

Immunofluorescence staining and confocal microscopy

Formalin-fixed and paraffin-embedded skin biopsies were cut into 3-μm thick sections, deparaffinized, and blocked using donkey serum. The following primary antibodies were used: rabbit anti-LC3B (Novus Biologicals, Centennial, CO), goat anti-LC3C (Abcam, Cambridge, United Kingdom), mouse anti−SARS-CoV-2 spike (GeneTex, Irvine, CA), rabbit anti-VEGF (Abcam), goat anti-myeloperoxidase (R&D Systems, Minneapolis, MN), rabbit anti-LL37 (Novus Biologicals), mouse anti-CD31 (Dako, Waltham, MA), or mouse anti-CD163 (DCS Diagnostics, Hamburg, Germany). Bound mAb was visualized using Cy3 donkey anti-rabbit antibody, Alexa 647 donkey anti-rabbit antibody, Alexa 488 donkey anti-goat antibody, Alexa647-donkey-anti-mouse antibody, Cy3-donkey-anti-human antibody (Dianova, Hamburg, Germany). For nuclear staining, we used DAPI (Sigma-Aldrich). Immunofluorescence images were obtained with a confocal laser scanning microscope LSM 800 (Carl Zeiss), and images were processed and analyzed with ZEN Blue software, version 2.6.

Calu-3 cells were infected with SARS-CoV-2 (Tü1, multiplicity of infection of 0.06) or treated with cell supernatant of SARS-CoV-2 spike−transfected human epidermal keratinocyte 293T cells. For the latter, human epidermal keratinocyte 293T cells were transfected with 2 μg pCG-SARS-2-S using polyethyleneimine. After 16 hours, the medium was changed, and 48 hours after the medium change, the cell supernatant was harvested. The supernatant was cleared from dead cells and cell debris at 2,600*g* for 7 minutes. Secreted protein and microvesicles were concentrated by centrifugation for 2 hours at 21,000*g* and 4 °C. After aspirating the supernatant, the pellet was resuspended in DMEM, supplemented with 5% fetal calf serum, and added to Calu-3 cells. Thirty-six hours after SARS-CoV-2 infection or cell supernatant treatment, Calu-3 cells were detached, washed with PBS, fixed with 4% paraformaldehyde, and stored in 1% fetal calf serum. After centrifugation at 400*g*, the cell pellets were cut into 5-μm thick sections on the cryostat. Frozen sections were blocked using donkey serum and then incubated with the primary antibodies rabbit anti-LC3B (Novus Biologicals), goat anti-LC3C (Abcam), and mouse anti−SARS-CoV-2 spike (GeneTex). Bound mAbs were visualized using the same antibodies described earlier.

Data availability statement

All data generated or used during the study appear in the submitted article.

ORCIDs

Andrea Gawaz: http://orcid.org/0000-0002-3104-8539
Emmanuella Guenova: http://orcid.org/0000-0001-5478-8735
Stephan Forchhammer: http://orcid.org/0000-0002-1274-2613
Birgit Fehrenbacher: http://orcid.org/0000-0003-3022-7567
Anneli Vollert: http://orcid.org/0009-0000-5191-8709
Simon Riel: http://orcid.org/0000-0002-6618-9905
Michael Schindler: http://orcid.org/0000-0001-8989-5813
Elena Hagelauer: http://orcid.org/0009-0002-4004-1846
Luisa Unterluggauer: http://orcid.org/0000-0002-0805-9301
Isabella Pospischil: http://orcid.org/0000-0002-9427-1674
Wolfram Hoetzenecker: http://orcid.org/0000-0003-4710-0642
Martin Schaller: http://orcid.org/0000-0002-7930-1919

CONFLICT OF INTEREST

SF reports honoraria from Recordati, Kyowa Kirin, and Takeda Pharmaceuticals and institutional grants from NeraCare, SkylineDX, and BioNTech outside this work. The authors state no conflict of interest.

ACKNOWLEDGMENTS

This work was supported by the European Academy of Dermatology and Venereology (PPRC-2019-20); funds from the Department of Dermatology, Medical University of Vienna; the MED-CALL from the Faculty of Medicine, Johannes Kepler University Linz; and the University of Lausanne (SKINTEGRITY.CH collaborative research program).

AUTHOR CONTRIBUTIONS

Conceptualization: AG, EG, SF, BF; Data Curation: SR, AV, BF, GB, MG, LU, GS, IP, WH, SF; Formal Analysis: MiS, MaS; Visualization: SR, AV, BF; Supervision: EG; Writing − Original Draft Preparation: AG, SF; Writing − Review and Editing: AG, EG, MaS, MiS, EH, GB, MG, LU, GS, IP, WH, SF

SUPPLEMENTARY MATERIAL

Supplementary material is linked to the online version of the paper at www.jidonline.org, and at https://doi.org/10.1016/j.jid.2023.07.018.

REFERENCES

Bartolomeo CS, Lemes RMR, Morais RL, Pereria GC, Nunes TA, Costa AJ, et al. SARS-CoV-2 infection and replication kinetics in different human cell types: the role of autophagy, cellular metabolism and ACE2 expression. Life Sci 2022;308:120930.

Becker RC. COVID-19-associated vasculitis and vasculopathy. J Thromb Thrombolysis 2020;50:499−511.

Bischoff ME, Zang Y, Chu J, Price AD, Ehmer B, Talbot NJ, et al. Selective MAP1LC3C (LC3C) autophagy requires noncanonical regulators and the C-terminal peptide. J Cell Biol 2021;220:e202004182.

Bradley BT, Maioli H, Johnston R, Chaudhry I, Fink SL, Xu H, et al. Histopathology and ultrastructural findings of fatal COVID-19 infections in Washington State: a case series [published correction appears in Lancet 2020;396:312] Lancet 2020;396:320−32.

Caputo V, Metze D, Bonoldi E, Merli M, Rongioletti F. Peculiar histopathologic feature of an erythematous/morbilliform eruption in a COVID-19-positive patient. Am J Dermatopathol 2021;43:962−4.

Carlson JA. The histological assessment of cutaneous vasculitis. Histopathology 2010;56:3−23.

Coelho PP, Hesketh GG, Pedersen A, Kuzmin E, Fortier AN, Bell ES, et al. Endosomal LC3C-pathway selectively targets plasma membrane cargo for autophagic degradation. Nat Commun 2022;13:3812.

Colmenero I, Santonja C, Alonso-Riaño M, Noguera-Morel L, Hernández-Martín A, Andina D, et al. SARS-CoV-2 endothelial infection causes COVID-19 chilblains: histopathological, immunohistochemical and ultrastructural study of seven paediatric cases. Br J Dermatol 2020;183:729−37.

Daneshgaran G, Dubin DP, Gould DJ. Cutaneous manifestations of COVID-19: an evidence-based review. Am J Clin Dermatol 2020;21:627−39.

Decout A, Katz JD, Venkatraman S, Ablasser A. The cGAS-STING pathway as a therapeutic target in inflammatory diseases. Nat Rev Immunol 2021;21:548−69.

Deinhardt-Emmer S, Böttcher S, Häring C, Giebeler L, Henke A, Zell R, et al. SARS-CoV-2 causes severe epithelial inflammation and barrier dysfunction. J Virol 2021;95:e00110−21.

Dittmayer C, Laue M. Continued false-positive detection of SARS-CoV-2 by electron microscopy. Ann Neurol 2022;92:340−1.

Dittmayer C, Meinhardt J, Radbruch H, Radke J, Heppner BI, Heppner FL, et al. Why misinterpretation of electron micrographs in SARS-CoV-2-infected tissue goes viral. Lancet 2020;396:e64−5.

Dolhnikoff M, Ferreira Ferranti J, de Almeida Monteiro RA, Duarte-Neto AN, Soares Gomes-Gouvêa M, Viu Degaspare N, et al. SARS-CoV-2 in cardiac tissue of a child with COVID-19-related multisystem inflammatory syndrome [published correction appears in Lancet child Adolesc Health 2020;4:e39] Lancet Child Adolesc Health 2020;4:790−4.

Domizio JD, Gulen MF, Saidoune F, Thacker VV, Yatim A, Sharma K, et al. The cGAS-STING pathway drives type I IFN immunopathology in COVID-19. Nature 2022;603:145−51.

Dou Q, Wei X, Zhou K, Yang S, Jia P. Cardiovascular manifestations and mechanisms in patients with COVID-19. Trends Endocrinol Metab 2020;31:893–904.

Ertuğlu LA, Kanbay A, Afşar B, Elsürer Afşar R, Kanbay M. COVID-19 and acute kidney injury. COVID-19 ve Akut böbrek hasar. Tuberk Toraks 2020;68:407–18.

Facchetti F, Bugatti M, Drera E, Tripodo C, Sartori E, Cancila V, et al. SARS-CoV2 vertical transmission with adverse effects on the newborn revealed through integrated immunohistochemical, electron microscopy and molecular analyses of Placenta. EBiomedicine 2020;59:102951.

Farkash EA, Wilson AM, Jentzen JM. Ultrastructural evidence for direct renal infection with SARS-CoV-2 [published correction appears in J Am Soc Nephrol 2020;31:2494] J Am Soc Nephrol 2020;31:1683–7.

Galván Casas C, Català A, Carretero Hernández G, Rodríguez-Jiménez P, Fernández-Nieto D, Rodríguez-Villa Lario A, et al. Classification of the cutaneous manifestations of COVID-19: a rapid prospective nationwide consensus study in Spain with 375 cases. Br J Dermatol 2020;183:71–7.

García-Gil MF, Monte Serrano J, García García M, Barra Borao V, Matovelle Ochoa C, Ramirez-Lluch M, et al. Acral purpuric lesions associated with coagulation disorders during the COVID-19 pandemic. Int J Dermatol 2020;59:1151–2.

Garrido Ruiz MC, Santos-Briz Á, Santos-Briz Á, Sánchez A, Alonso-Riaño M, Burgos J, et al. Spectrum of clinicopathologic findings in COVID-19-induced skin lesions: demonstration of direct viral infection of the endothelial cells. Am J Surg Pathol 2021;45:293–303.

Gassen NC, Papies J, Bajaj T, Emanuel J, Dethloff F, Chua RL, et al. SARS-CoV-2-mediated dysregulation of metabolism and autophagy uncovers host-targeting antivirals. Nat Commun 2021;12:3818.

Gawaz A, Guenova E. Microvascular skin manifestations caused by COVID-19. Hamostaseologie 2021;41:387–96.

Hernández-Fernández F, Sandoval Valencia H, Barbella-Aponte RA, Collado-Jiménez R, Ayo-Martín Ó, Barrena C, et al. Cerebrovascular disease in patients with COVID-19: neuroimaging, histological and clinical description. Brain 2020;143:3089–103.

Hopfer H, Herzig MC, Gosert R, Menter T, Hench J, Tzankov A, et al. Hunting coronavirus by transmission electron microscopy - a guide to SARS-CoV-2-associated ultrastructural pathology in COVID-19 tissues. Histopathology 2021;78:358–70.

Hu J, Liu K. Complete and incomplete hepatitis B virus particles: formation, function, and application. Viruses 2017;9:56.

Hwang HJ, Ha H, Lee BS, Kim BH, Song HK, Kim YK. LC3B is an RNA-binding protein to trigger rapid mRNA degradation during autophagy. Nat Commun 2022;13:1436.

Khandia R, Dadar M, Munjal A, Dhama K, Karthik K, Tiwari R, et al. A comprehensive review of autophagy and its various roles in infectious, non-infectious, and lifestyle diseases: current knowledge and prospects for disease prevention, novel drug design, and therapy. Cells 2019;8:674.

Ko CJ, Harigopal M, Gehlhausen JR, Bosenberg M, McNiff JM, Damsky W. Discordant anti-SARS-CoV-2 spike protein and RNA staining in cutaneous perniotic lesions suggests endothelial deposition of cleaved spike protein. J Cutan Pathol 2021;48:47–52.

Lange K, Matthies M, Firouzi-Memarpuri P, Homey B. [COVID-19 and skin manifestations: overview of current literature]. Hautarzt 2022;73:291–7.

Madjo U, Leymarie O, Frémont S, Kuster A, Nehlich M, Gallois-Montbrun S, et al. LC3C contributes to Vpu-mediated antagonism of BST2/tetherin restriction on HIV-1 release through a non-canonical autophagy pathway. Cell Rep 2016;17:2221–33.

Magro C, Mulvey JJ, Berlin D, Nuovo G, Salvatore S, Harp J, et al. Complement associated microvascular injury and thrombosis in the pathogenesis of severe COVID-19 infection: a report of five cases. Transl Res 2020;220:1–13.

Magro C, Nuovo G, Mulvey JJ, Laurence J, Harp J, Crowson AN. The skin as a critical window in unveiling the pathophysiologic principles of COVID-19. Clin Dermatol 2021;39:934–65.

Maier HJ, Cottam EM, Stevenson-Leggett P, Wilkinson JA, Harte CJ, Wileman T, et al. Visualizing the autophagy pathway in avian cells and its application to studying infectious bronchitis virus. Autophagy 2013;9:496–509.

Marzano AV, Cassano N, Genovese G, Moltrasio C, Vena GA. Cutaneous manifestations in patients with COVID-19: a preliminary review of an emerging issue. Br J Dermatol 2020b;183:431–42.

Marzano AV, Genovese G, Fabbrocini G, Pigatto P, Monfrecola G, Piraccini BM, et al. Varicella-like exanthem as a specific COVID-19-associated skin manifestation: multicenter case series of 22 patients. J Am Acad Dermatol 2020a;83:280–5.

Negrini S, Guadagno A, Greco M, Parodi A, Burlando M. An unusual case of bullous haemorrhagic vasculitis in a COVID-19 patient. J Eur Acad Dermatol Venereol 2020;34:e675–6.

Nehls J, Businger R, Hoffmann M, Brinkmann C, Fehrenbacher B, Schaller M, et al. Release of immunomodulatory Ebola virus glycoprotein-containing microvesicles is suppressed by tetherin in a species-specific manner. Cell Rep 2019;26:1841–53.e6.

Nuno-Gonzalez A, Martin-Carrillo P, Magaletsky K, Martin Rios MD, Herranz Mañas C, Artigas Almazan J, et al. Prevalence of mucocutaneous manifestations in 666 patients with COVID-19 in a field hospital in Spain: oral and palmoplantar findings. Br J Dermatol 2021;184:184–5.

Pinheiro da Silva F, Medeiros MC, Dos Santos ÂB, Ferreira MA, Garippo AL, Chammas R, et al. Neutrophils LL-37 migrate to the nucleus during overwhelming infection. Tissue Cell 2013;45:318–20.

Roden AC, Vrana JA, Koepplin JW, Hudson AE, Norgan AP, Jenkinson G, et al. Comparison of in situ hybridization, immunohistochemistry, and reverse transcription-droplet digital polymerase chain reaction for severe acute respiratory syndrome coronavirus 2 (SARS-CoV-2) testing in tissue. Arch Pathol Lab Med 2021;145:785–96.

Ruetalo N, Businger R, Althaus K, Fink S, Ruoff F, Pogoda M, et al. Antibody response against SARS-CoV-2 and seasonal coronaviruses in nonhospitalized COVID-19 patients. mSphere 2021;6:e01145–220.

Shams S, Rathore SS, Anvekar P, Sondhi M, Kancherla N, Tousif S, et al. Maculopapular skin eruptions associated with Covid-19: a systematic review. Dermatol Ther 2021;34:e14788.

Unterluggauer L, Pospischil I, Krall C, Saluzzo S, Kimeswenger S, Karolyi M, et al. Cutaneous manifestations of SARS-CoV-2: a 2-center, prospective, case-controlled study. J Am Acad Dermatol 2021;85:202–4.

Varga Z, Flammer AJ, Steiger P, Haberecker M, Andermatt R, Zinkernagel AS, et al. Endothelial cell infection and endotheliitis in COVID-19. Lancet 2020;395:1417–8.

Welsh E, Cardenas-de la Garza JA, Brussolo-Marroquín E, Cuellar-Barboza A, Franco-Marquez R, Ramos-Montañez G. Negative SARS-CoV-2 antibodies in patients with positive immunohistochemistry for spike protein in Pityriasis rosea-like eruptions. J Eur Acad Dermatol Venereol 2022;36:e661–2.

Wrapp D, Wang N, Corbett KS, Goldsmith JA, Hsieh CL, Abiona O, et al. Cryo-EM structure of the 2019-nCoV spike in the prefusion conformation. Science 2020;367:1260–3.

Zhao Q, Fang X, Pang Z, Zhang B, Liu H, Zhang F. COVID-19 and cutaneous manifestations: a systematic review. J Eur Acad Dermatol Venereol 2020;34:2505–10.

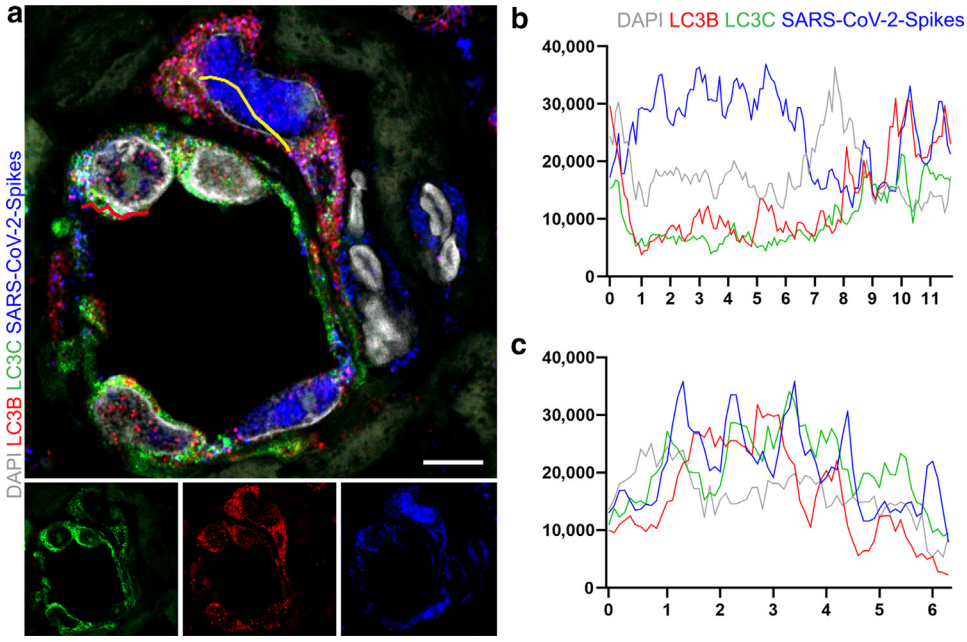

Supplementary Figure S1. Confocal immunofluorescence—dermal microvascular cells in COVID-19. (**a**) Stained for LC3B (red), LC3C (green), SARS-CoV-2 spikes (blue), and nuclei DAPI (gray). (**b**) Yellow and (**c**) red line graphs visualizing cellular localization. SARS-CoV-2, severe acute respiratory syndrome coronavirus 2.

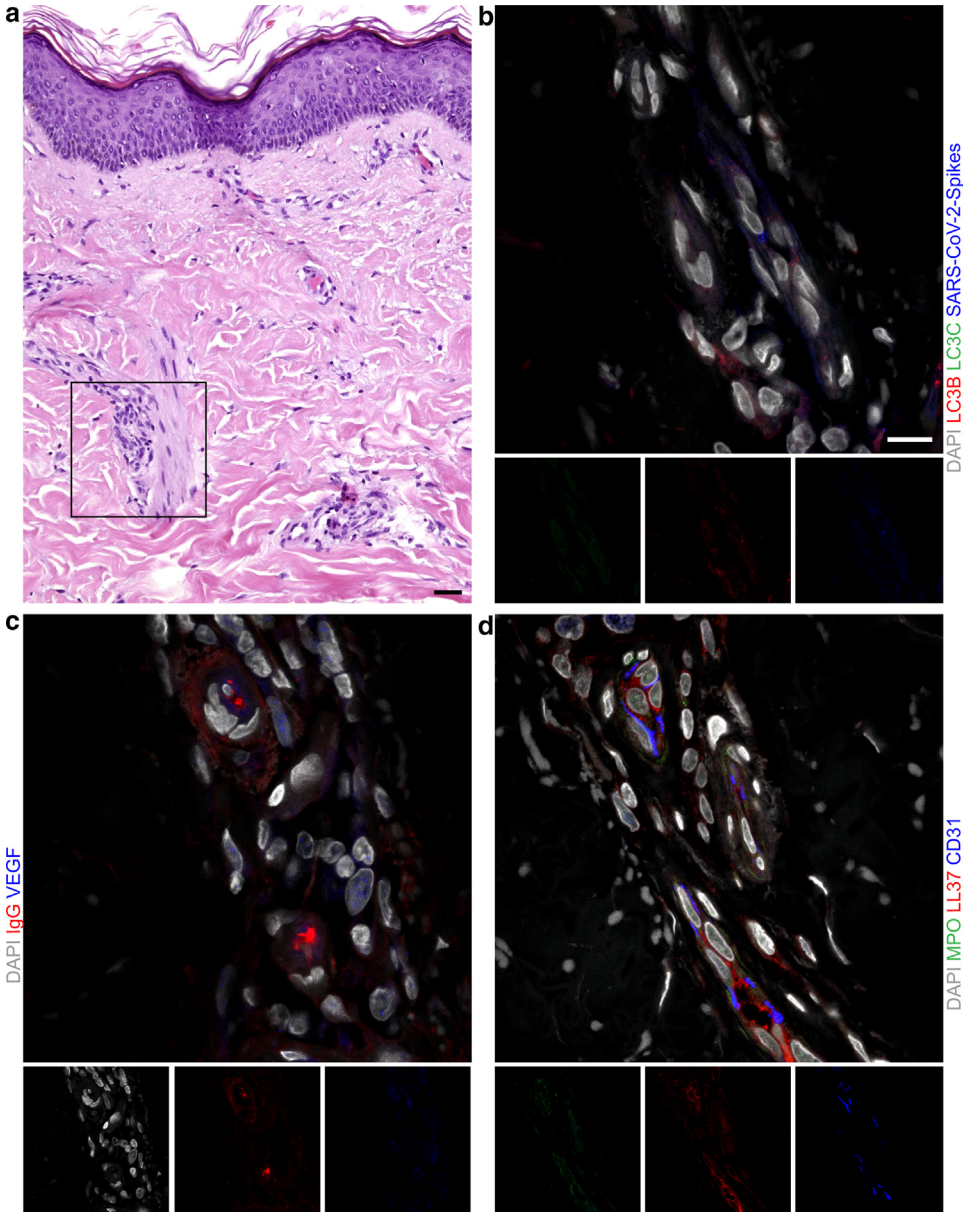

Supplementary Figure S2. Confocal immunofluorescence—dermal microvascular cells in normal skin vessels. Representative serial sections of one normal skin sample with diverse stainings are shown. (**a**) H&E overview, square marking the same vessel seen in **b**, **c**, and **d**. (**b**) LC3B (red), LC3C (green), and SARS-CoV-2 spikes (blue). (**c**) IgG (red) and VEGF (blue). (**d**) MPO (green), LL37 (red), and CD31 (blue). DAPI (gray) was used for nuclear staining (for **b**–**d**). Bar in **a** = 10 μm and **b** = 50 μm. MPO, myeloperoxidase; SARS-CoV-2, severe acute respiratory syndrome coronavirus 2.

Supplementary Figure S3. Confocal immunofluorescence—dermal microvascular cells in vasculitis. Representative serial sections of one non–COVID-19 vasculitis skin sample with diverse stainings are shown. (**a**) H&E overview, square marking the same vessel seen in **b**, **c**, and **d**. (**b**) LC3B (red), LC3C (green), and SARS-CoV-2 spikes (blue). (**c**) IgG (red), VEGF (blue). (**d**) MPO (green), LL37 (red), CD31 (blue). DAPI (gray) was used for nuclear staining (**b**–**d**). Bar in **a** = 10 μm and **b** = 50 μm. SARS-CoV-2, severe acute respiratory syndrome coronavirus 2.

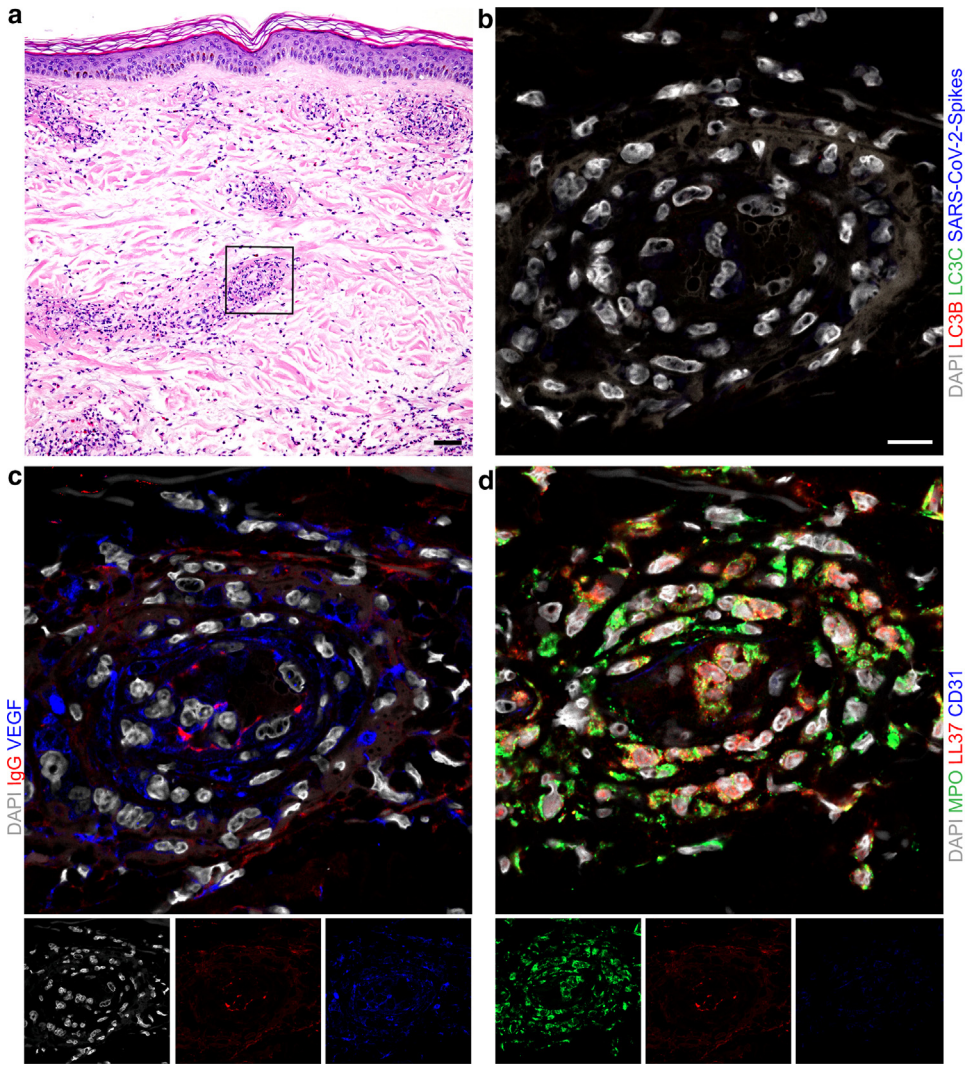

Supplementary Table S1. Characteristics of the Cohort

Patient Number	Age (y)	Sex	Biopsy Localization	Comorbidities	Course of Disease
COVID-19 with vasculitis					
1	62	M	Ankle	Lung transplantation in 2004, immunocompromised, intraductal papillary, mucinous neoplasm	Severe
2	23	M	Inguinal	None	Mild
3	22	M	Thorax	None	Severe
4	46	M	Back	None	Moderate
COVID-19 without vasculitis					
5	64	M	Thorax	None	Mild
6	66	M	Upper leg	None	Moderate
7	51	M	Upper leg	None	Mild
8	59	M	Upper arm	Diabetes mellitus	Moderate
9	43	F	Lower leg	None	Mild
10	20	M	Upper leg	None	Moderate
11	21	F	Buttocks	Chronic vertigo	Moderate
12	56	M	Abdomen	None	Mild
13	42	F	Thorax	None	Moderate
14	65	F	Upper leg	Cardiovascular disease; diabetes mellitus	Mild
15	58	M	Buttocks	Primary cutaneous marginal zone B-cell lymphoma	Mild
16	67	F	Abdomen	Cardiovascular disease	Mild
17	32	F	Lower leg	Sjögren syndrome; immunocompromised	Mild
18	25	F	Lower leg	Paroxysmal spells	Mild
19	20	F	Buttocks	None	Moderate
20	19	M	Abdomen	Atopic dermatitis	Moderate
21	47	M	Lower leg	Cardiovascular disease	Mild
22	32	M	Upper leg	None	Mild
23	48	M	Back	None	Moderate
24	34	F	Back	Mycosis fungoides	Moderate
25	53	F	Abdomen	None	Mild
Non–COVID-19 vasculitis control					
26	41	F	Lower leg	Urinary tract infection	n/a
27	67	F	Lower leg	Glaucoma	n/a
28	68	F	Buttocks	Chronic gastritis, degenerative spinal changes	n/a

Abbreviations: F, female; M, male; n/a, not applicable.